Article ID: 1003－6326(2005)04－0727－06

Effect of carbon addition on microstructure and mechanical properties of Ti-based bulk metallic glass forming alloys①

SUN Yu-feng(孙玉峰)[1,2], WANG Yu-ren(王育人)[1],
WEI Bing-chen(魏炳忱)[1], LI Wei-huo(李维火)[1], SHEK Chung-hong(石灿鸿)[2]
(1. National Microgravity Laboratory, Institute of Mechanics,
Chinese Academy of Sciences, Beijing 100080, China;
2. Department of Physics and Materials Science, City University of Hong Kong,
Hong Kong)

Abstract: A kind of novel Ti-based composites was developed by introducing different amounts of carbon element to the $Ti_{50}Cu_{23}Ni_{20}Sn_7$ bulk metallic glass forming alloys. The thermal stability and microstructural evolution of the composites were investigated. Room temperature compression tests reveal that the composite samples with 1% and 3%(mass fraction) carbon additions have higher fracture strength and obvious plastic strain of 2 195 MPa, 3.1% and 1 913 MPa, 1.3% respectively, compared with those of the corresponding carbon-free $Ti_{50}Ni_{20}Cu_{23}Sn_7$ alloys. The deformation mechanisms of the composites with improved mechanical properties were also discussed.

Key words: casting; bulk metallic glasses; Vein pattern; mechanical properties; composites
CLC number: TG 139.8 **Document code:** A

1 INTRODUCTION

Bulk metallic glasses(BMGs) have attracted great attention due to their unique properties, for example, superior strength and high hardness, excellent corrosion resistance and high wear resistance. However, the high strength of BMGs is often accompanied by remarkably little global plasticity due to the highly localized shear band formed during the deformation process[1-4]. Some BMGs are very robust against heterogeneous nucleation at the surface or interface during the melting process, which leads to the development of a kind of novel materials, BMG matrix composites. Up to now, the fabrication of BMG matrix composites is still considered to be the most appropriate way to increase the plastic deformation of BMGs. Generally speaking, BMG matrix composites can be reinforced by adding refractory ceramics such as SiC or WC, ductile metals such as Nb or Ta and fibres such as C and steel, which result in improved plastic deformation and greatly expand the potential application of BMGs[5-9].

As traditional structural and engineering materials, Ti-based alloys are extensively used in many areas due to their low density and excellent mechanical properties, especially aeronautic and automobile applications. In recent years, Ti-based BMGs were successfully synthesized and exhibited a high tensile strength of up to 2 200 MPa[10]. However, the glass-forming ability for Ti-based BMGs is not as high as that for Zr- or Pa-based BMGs and millimeters-sized Ti-based BMGs are seldom reported to be developed. One of the largest glass-forming ability of Ti-based BMGs is $Ti_{50}Cu_{23}Ni_{20}Sn_7$, which is developed by Zhang and Inoue in 1998[11]. Moreover, the composition modification of $Ti_{50}Cu_{23}Ni_{20}Sn_7$ alloys leads to developing a kind of new Ti-based composite with the microstructure of dendrite/(glass+ crystal) matrix or dendrite/nanostructure matrix, which shows a promising combination of high strength, pronounced stain hardening and large plastic strains under compression[12-15].

It was reported that the small size atom additions play an important role in the GFA of the alloy system, and the addition tends to suppress the large-scale diffusion and crystallization in the supercooled liquid state. In this paper, the composites were designed by introducing different amounts of carbon element into the $Ti_{50}Cu_{23}Ni_{20}Sn_7$ alloy. The microstructure, thermal stability and compressive deformation characteristics are investigated. It is revealed that the introduction of carbon

① **Foundation item:** Project(KJCX2-SW-L05) supported by the Knowledge Innovation Program of Chinese Academy of Sciences; project (50101012) supported by the National Natural Science Foundation of China
Received date: 2004－11－08; **Accepted date:** 2005－01－24
Correspondence: WANG Yu-ren, Professor; Tel: +86-10-62614945; E-mail: wangyr@imech.ac.cn

element make it possible to develop high strength Ti-base composites with good plasticity.

2 EXPERIMENTAL

The BMG forming alloys with a nominal composition of $Ti_{50}Cu_{23}Ni_{20}Sn_7$ were prepared by directly arc melting a mixture of pure Ti, Cu, Ni and Sn metals with a purity of about 99.9% in a Ti-gettered argon atmosphere to form button ingots. The button ingots were then smashed into μm-sized particles and uniformly mixed with 99% pure carbon powders. The mass fraction of the carbon addition was 1% and 3% respectively. Subsequently the mixtures were melted in a high vacuum electric resistance furnace to form carbon-bearing ingots. The carbon-bearing ingots were again arc melted and suction cast into a water-cooled copper mold to form 7 mm long alloy rods with diameter of 1, 2 and 3 mm respectively. For comparison, thin ribbons with the same composition and a thickness of about 20 μm were prepared by single copper wheel melt spinning.

All the ribbons and rods were studied by differential scanning calorimetry (DSC) at constant heating rate of 20 K/min in a flowing argon atmosphere using a Perkin-Elmer DSC7 calorimeter. The structure of the melt-spun ribbons and as-cast alloy rods were investigated by X-ray diffraction (XRD) using a Philips PW 1050 diffractometer with Cu K_α radiation. Field emission scanning electron microscopy (FESEM) (Jeol JSM-6400LV microscope) was used for the analysis of the microstructure and for characterization of fracture surfaces. SEM electron microprobe analysis was used to determine the phase composition. The room temperature compressive properties of the d3 mm as-cast alloy rods with the aspect ratio of 2∶1 were tested using an Instron 5567 testing machine at a strain rate of 1×10^{-4}/s.

3 RESULTS AND DISCUSSION

The X-ray diffraction was used to analyze the phase constitutes of the melt-spun ribbons as well as the as-cast composite rods. The typical XRD patterns are shown in Fig. 1. It is shown that the XRD patterns of the melt-spun ribbons display no distinct crystalline diffraction peak, indicating the formation of an amorphous phase. For alloy rods with diameter equal to or larger than 1 mm, the diffraction peak of crystalline phase can be found from the XRD patterns, which also implies the severe conditions required to fabricate monolithic Ti-based BMG. For d1 mm rods, a small crystalline diffraction peak that was identified to be β-Ti was found imposed on the broad diffraction peak. The intensity of the crystalline diffraction peak increases with the increasing carbon additions. For alloy rods with diameter larger than 1 mm, which corresponds to slower cooling rate, the diffraction peaks of Ti_3Sn and Ti_2Ni phase were also found from the XRD patterns. For the alloy rods with the same diameter, the increasing carbon addition to the $Ti_{50}Cu_{23}Ni_{20}Sn_7$ BMG forming alloys not only contributes to the diffraction peaks of TiC, but also leads to the increasing intensity of the Ti_3Sn diffraction peaks.

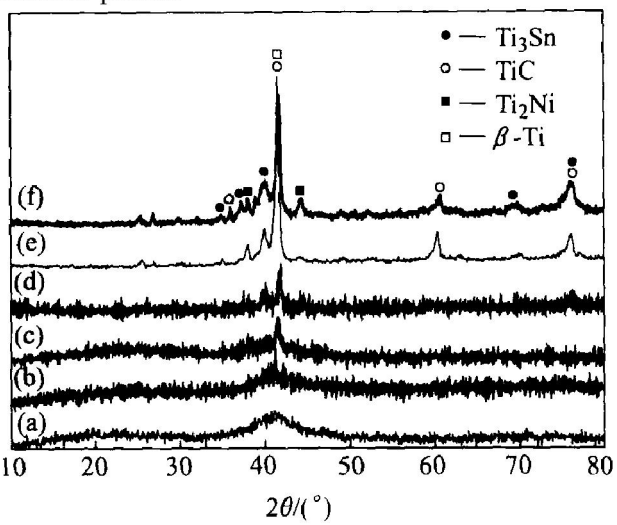

Fig. 1 XRD patterns of melt-spun $Ti_{50}Cu_{23}Ni_{20}Sn_7$ ribbons and as-cast rods with different amounts of carbon addition
(a) —Ribbon, x= 0; (b) —d= 1 mm, x= 0; (c) —d= 1 mm, x= 1%; (d) —d= 2 mm, x= 1%; (e) —d= 2 mm, x= 3%; (f) —d= 3 mm, x= 3%
(x is the mass fraction of carbon)

DSC analyses carried out for the melt-spun ribbons and as-cast rods are shown in Fig. 2. For melt-spun ribbons, all the samples exhibit two obvious exothermic peaks. With increasing carbon addition, the glass transition temperature T_g of the alloy, as well as the first and second crystallization peak T_{x1} and T_{x2} move to a higher temperature. While the temperature range of the supercooled liquid region doesn't seem to change a lot. However, the temperature interval between the first and second crystallization temperature decreases obviously by adding carbon elements. For the d 3 mm rods, the exothermic peaks are very weak and the variation of the glass transition temperature and the crystallization temperature with the carbon addition is similar to that of melt-spun ribbon, but the absolute value is quite small, indicating the major part of the samples being crystalline. For d3 mm rods with 3% carbon addition, no glass transition and crystallization peak can be found. By comparing the exothermic heat flow released during crystallization of the as-cast rods with that of

the melt-spun ribbons, the volume fraction of glass phase in the as-cast rods can be estimated as about 20% for the d 3 mm carbon-free alloy rods and about 10% for the d 3 mm cylinder containing 1% carbon addition.

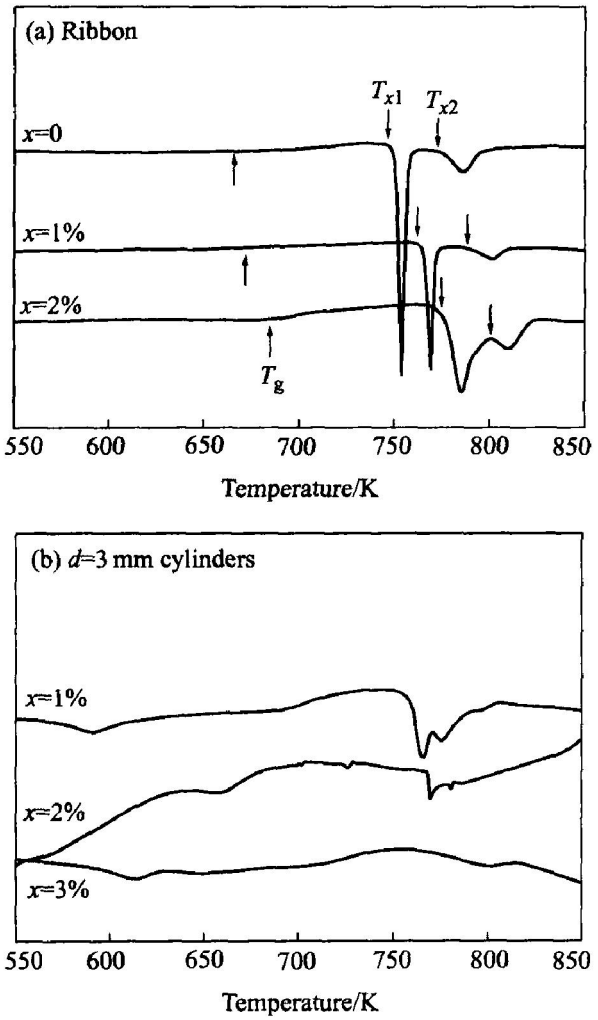

Fig. 2 DSC curves of $Ti_{50}Cu_{23}Ni_{20}Sn_7$ melt-spun ribbons(a) and as-cast d3 mm composite rods(b) (x represents the mass fraction of carbon in samples)

Fig. 3 shows the SEM images of the microstructure of the d3 mm as-cast $Ti_{50}Cu_{23}Ni_{20}Sn_7$ rods on cross-sections with different carbon additions. The microstructure of carbon-free alloy rod shown in Fig. 3(a) exhibits a microstructure with bright irregular shaped phase and very fine particles. The bright irregular shaped phase arrays in line and separates the whole matrix into different "parts" (gray-colored areas in the image) with the size of about 3 μm width and 10 μm length. The very fine particles are only densely distributed in some of the "parts", while in other "parts", no particles are found. EDX analysis reveals that the bright phase has a composition of $Ti_{60.91}Ni_{12.08}Cu_{13.61}Sn_{13.41}$, i. e. the Sn content is nearly two times of the average value. Combined with the result of XRD, the bright phase can be identified to be Ti_3Sn, solid soluted Cu and Ni elements. The matrix has a composition of $Ti_{49.69}Ni_{21.47}Cu_{23.04}Sn_{5.81}$, which is similar to the original composition. It is obvious that a part of the matrix has transformed from amorphous state to β-Ti(Ni, Cu) solid solute. As for the very fine particles, the size is too small to be analyzed by EDX. However, their volume fraction is big enough for XRD detection, which proves it to be Ti_2Ni phase. The precipitation of Ti_2Ni and Ti_3Sn particles has changed the matrix composition. Fig. 3(b) shows the microstructure of the rod with 1% carbon addition. The TiC particles, with the size of about 2 μm, formed via reaction Ti+ C $\rightarrow$ TiC are found, which is indicated by the white arrow. Compared with the microstructure of carbon-free $Ti_{50}Cu_{23}Ni_{20}Sn_7$ rods, the microstructure of the rod with 1% carbon addition shows that the second phase particles distribute more uniformly in the matrix. The in-situ formed TiC particles prevent the Ti_3Sn from arraying aggregatively in line. In contrast Ti_3Sn distribute randomly in the matrix. The matrix is also kept out of being separated into large "parts" and retains its continuity. For the microstructure of the rod with 3% carbon addition shown in Fig. 3(c), more and larger TiC particles with the size of about 5 μm can be found to be distributed on the matrix, together with bright Ti_3Sn intermetallic compound and nano-sized Ti_2Ni particles. Fig. 3(d) shows the interface between TiC and the matrix at higher magnification. A layer with 50 nm thickness is found at the interface, which is proved by EDXS analysis to be Ti_3Sn. It seems that the presence of TiC can act as the nucleation site for the Ti_3Sn phase. The precipitation of large amount of crystalline phase causes the formation of crack on the matrix, which is indicated by the arrows shown in Fig. 3(c). The crack may be formed during the cooling process due to the different physical properties between the matrix and the precipitates. The presence of crack also indicates the deterioration of the mechanical properties of the alloys.

A series of compression tests have been carried out for the d3 mm as-cast Ti-base alloy rods at room temperature. Fig. 4 shows the typical stress—strain curves. For the carbon-free alloy rods, the ultimate compression stress reaches 1 936 MPa with nearly zero plastic strain for the sample. For the rods with 1% carbon addition, yielding occurs at about 1 160 MPa, followed by "work hardening" stage. The ultimate compression stress is 2 195 MPa and the plastic strain reaches about 3. 1%. With 3% carbon addition, there is a similar yielding and "work hardening" behavior like that of rods with 1% carbon addition. However, the ultimate compression stress is less, with the value of about 1 913 MPa. And the plastic strain of about 1. 3% is obtained before failure.

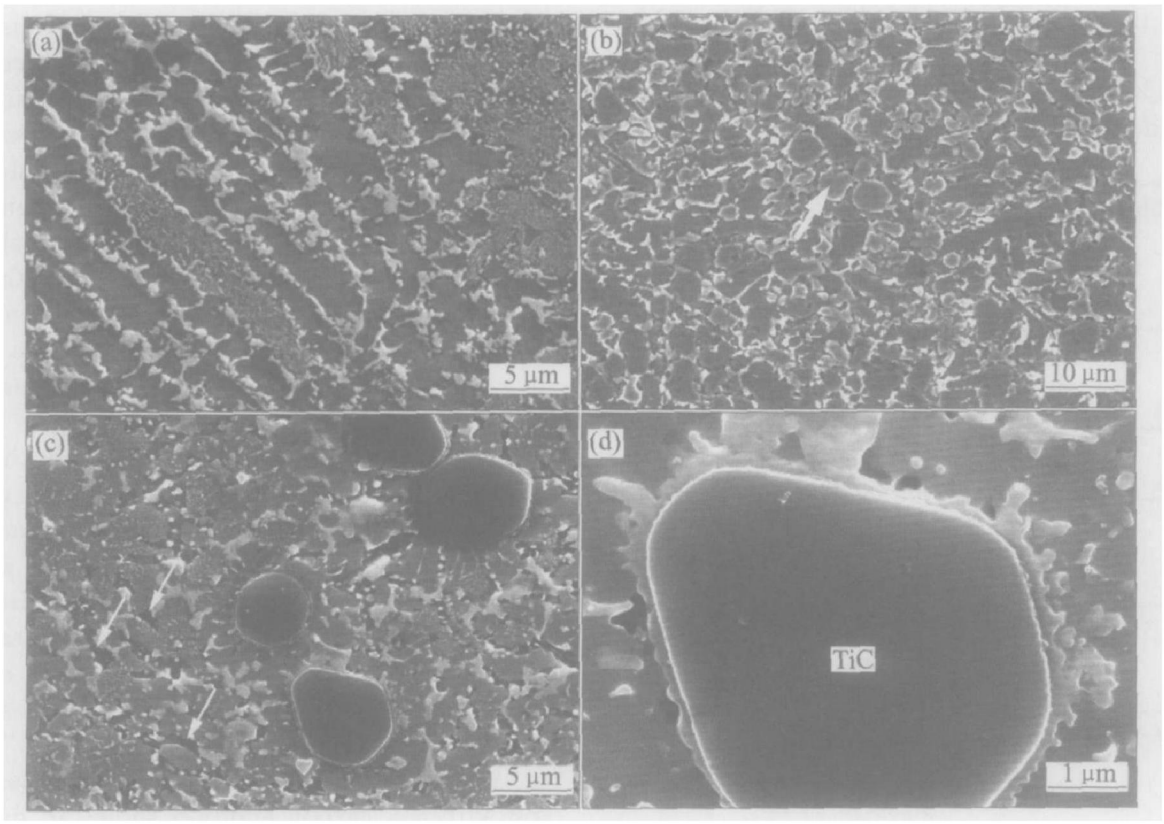

Fig. 3 SEM images of microstructures on cross-section of d3mm as-cast $Ti_{50}Cu_{23}Ni_{20}Sn_7$ rods
(a) —Carbon-free; (b) —1% carbon; (c), (d) —3% carbon

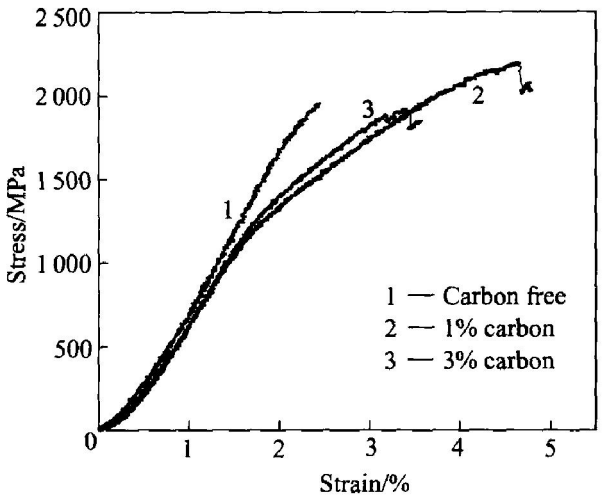

Fig. 4 Room temperature compressive stress—strain curves of d3 mm as-cast $Ti_{50}Cu_{23}Ni_{20}Sn_7$ rods

For the d3 mm as-cast rods with various carbon additions, the fracture occurs roughly along the maximum stress plane during compression, but none of the fracture plane is along about 45° with the loading direction. The SEM images of the fracture feature observation of d3 mm samples are shown in Fig. 5, which exhibit more complex fractured surfaces compared to monolithic BMGs. For carbon-free $Ti_{50}Cu_{23}Ni_{20}Sn_7$ rod, the fractured surface is composed of several fractured planes, as shown in Fig. 5(a). Although there are glass phase and crystalline phase, there is no obvious evidence of interaction between the shear bands and the crystalline and no plastic deformation appears in the materials. The Ti_2Ni particles are reported to be a brittle phase and can significantly reduce the ductility of the as-cast samples. Vein pattern are found along the shear-off direction of the fracture. The liquid-like droplets are observed in some regions of the fracture surface, indicating the high elastic deformation behavior of the glass phase of the material. The very fast concentration of the elastic energy in the shear bands leads to temperature rise to about several tens Kelvin in a very short time and causes the amorphous matrix to be remelted. For as-cast alloy rods with 1% carbon addition, the fractured surface is shown in Fig. 5 (b). Vein pattern cannot be clearly found on the fractured plane due to the little volume fraction of glass phase. However, some liquid-like region can be observed, as shown by an arrow in Fig. 5(b). In the area near the liquid-like region, many protuberances can be found on the fractured surface. The existence of the protuberances is believed to contribute to the large plasticity of the material, which is formed by the squeezing between the glass phase and the ductile β-Ti phase during the deformation process. From the microstructure observation shown in Fig. 3(b), it can be found that the matrix containing a great amount of Ti_3Sn metallic

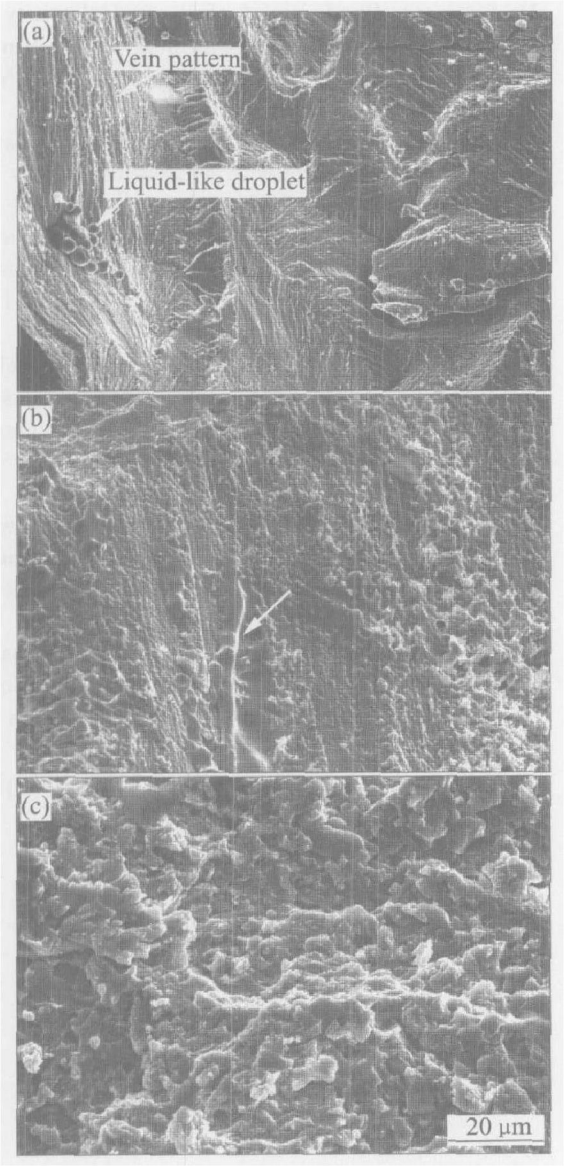

Fig. 5 SEM images showing fracture surfaces of d3 mm as-cast Ti-base alloy rods
(a) —Carbon free; (b) —1% carbon; (c) —3% carbon

compound is successive and forms a network structure. So for this sample, it shows more plastic deformation than the monolithic $Ti_{50}Cu_{23}Ni_{20}Sn_7$ cylinders. The more plastic deformation is due to the uniformly distributed crystalline phases at the matrix. The crystalline phase can interact with the deformation of the ductile β phase, which also leads to the work hardening behavior under loading. When the carbon addition increases to 3%, the fracture surface of the sample exhibits a rugged and dimple-like structure, which is similar to the fractography of the nanocrystalline + glass/dendrite crystalline composites and the nanocrystalline/dendritic crystalline composites. This may be attributed to the existence of the micrometer-sized Ti_3Sn particles and very fine Ti_2Ni precipitates in the matrix[16]. In this alloy, no detectable glass phase is found. Its microstructure is composed of β-Ti(Ni, Cu) phase, Ti_3Sn and Ti_2Ni metallic compound and TiC particles. The β-Ti(Ni, Cu) solute solid is the soft phase and contributes to the plastic deformation of the materials. Ti_3Sn is said to have only a small effect on the deformation process, while the Ti_2Ni is a brittle phase and is believed to deteriorate the plasticity[14]. And the particles are too densely distributed at the matrix, the distance between the particles will become very small, which makes it difficult for the plastic deformation to move through the materials, and thus, decreases the plasticity[17].

4 CONCLUSIONS

The $Ti_{50}Cu_{23}Ni_{20}Sn_7$ BMG forming alloys with different amounts of carbon addition were developed by copper mold casting. The solidified microstructural homogeneity strongly depends on the carbon additions. For carbon-free alloy rods, the imhomogeneously distrubuted Ti_3Sn intermetallic compound separates the matrix into large "parts". While the addition of carbon promotes the formation of Ti_3Sn and avoids the separation of matrix. However, the increasing carbon addition induces the formation of cracks on the matrix due to the precipitation of large amount of crystalline phase. The great microstructure evolution of the Ti-base alloy with small addition of carbon element also reveals that the GFA of the Ti-base alloy strongly depends on the alloy composition.

Due to the microstructure variation of the samples with different carbon contents, the mechanical properties of the composites differ greatly from each other. Composite rods with 1% carbon addition show the largest plasticity of 3.1% and ultimate compression stress of 2 195 MPa under uniaxial compression test, while the rods without carbon addition show no global plasticity. When the carbon addition increases to 3%, the plastic strain of the samples decreases to 1.3% with the ultimate compression stress of about 1 913 MPa.

REFERENCES

[1] Zhang Z F, Eckert J, Schultz L. Difference in compressive and tensile fracture mechanisms of $Zr_{59}Cu_{20}Al_{10}Ni_8Ti_3$ bulk metallic glass [J]. Acta Mater, 2003, 51(4): 1167 - 1179.

[2] Hufnagel T C, El-Deiry P, Vinci R P. Development of shear band structure during deformation of a $Zr_{57}Ti_5Cu_{20}Ni_8Al_{10}$ bulk metallic glass [J]. Scripta Mater, 2000, 43(12): 1071 - 1075.

[3] Bian Z, He G, Chen G L. Investigation of shear bands under compressive testing for Zr-base bulk metallic glasses containing nanocrystals [J]. Scripta Mater, 2002, 46(6): 407 - 412.

[4] Liu C T, Heatherly L, Eaton D S, et al. Test environments and mechanical properties of Zr-base bulk amorphous alloys [J]. Metall Mater Trans, 1998, 29A (6): 1811.

[5] Conner D, Dandliker R B, Johnson W L. Mechanical properties of tungsten and steel fiber reinforced $Zr_{41.25}Ti_{13.75}Cu_{12.5}Ni_{10}Be_{22.5}$ metallic glass matrix composites [J]. Acta Mater, 1998, 46(17): 6089-6102.

[6] Szuecs F, Kim C P, Johnson W L. Mechanical properties of $Zr_{56.2}Ti_{13.8}Nb_{5.0}Cu_{6.9}Ni_{5.6}Be_{12.5}$ ductile phase reinforced bulk metallic glass composite [J]. Acta Mater, 2001, 49(9): 1507-1513.

[7] Kim C P, Busch R, Johnson W L. Processing of carbon-fiber-reinforced $Zr_{41.2}Ti_{13.8}Cu_{12.5}Ni_{10.0}Be_{22.5}$ bulk metallic glass composites [J]. Applied Physics Letters, 2001, 79(10): 1456-1458.

[8] Jiang Q C, Li X L, Wang H Y. Fabrication of TiC particulate reinforced magnesium matrix composites [J]. Scripta Mater, 2003, 48(6): 713-717.

[9] Xu Y K, Xu J. Ceramics particulate reinforced $Mg_{65}Cu_{20}Zn_5Y_{10}$ bulk metallic glass composites [J]. Scripta Mater, 2003, 49(9): 843-848.

[10] Inoue A. Stabilization of metallic supercooled liquid and bulk amorphous alloys [J]. Acta Mater, 2000, 48(1): 279.

[11] Zhang T, Inoue A. Thermal and mechanical properties of Ti-Ni-Cu-Sn amorphous alloys with a wide supercooled liquid region before crystallization [J]. Mater Trans JIM, 1998, 39(3): 1001.

[12] He G, Loser W, Eckert J. Enhanced plasticity in a Ti-based bulk metallic glass-forming alloy by in situ formation of a composite microstructure [J]. J Mater Res, 2002, 17(12): 3015-18.

[13] He G, Eckert J, Loser W. Novel Ti-base nanostructure-dendrite composite with enhanced plasticity [J]. Nature Mater, 2003, 2(1): 33-37.

[14] He G, Eckert J, Loser W. Stability, phase transformation and deformation behavior of Ti-base metallic glass and composites [J]. Acta Mater, 2003, 51(7): 1621-1631.

[15] He G, Loser W, Eckert J. Microstructure, mechanical properties, and fracture mechanism of as-cast $(Ti_{0.5}Cu_{0.25}Ni_{0.15}Sn_{0.05}Zr_{0.05})_{100-x}Mo_x$ composites [J]. Metall Mater Trans, 2004, 35A(5): 1591-1601.

[16] Kim W J, Ma D S, Jeong H G. Superplastic fow in a $Zr_{65}Al_{10}Ni_{10}Cu_{15}$ metallic glass crystallized during deformation in a supercooled liquid region [J]. Scripta Mater, 2003, 49(11): 1067-1073.

[17] Calin M, Eckert J, Schultz L. Improved mechanical behavior of Cu-Ti-based bulk metallic glass by in situ formation of nanoscale precipitates [J]. Scripta Mater, 2003, 48(6): 653-658.

(Edited by YUAN Sai-qian)